Journal of Solid State Chemistry 182 (2009) 2368–2373

Contents lists available at ScienceDirect

Journal of Solid State Chemistry

journal homepage: www.elsevier.com/locate/jssc

Strontium–copper selenite–chlorides: Synthesis and structural investigation

Peter S. Berdonosov *, Andrei V. Olenev, Valery A. Dolgikh

Department of Chemistry, Moscow State University, 119991 GSP-1, Leninskie Gory, 1 build. 3, Moscow, Russia

ARTICLE INFO

Article history:
Received 7 April 2009
Received in revised form
11 June 2009
Accepted 13 June 2009
Available online 21 June 2009

Keywords:
Selenite
Crystal structure
Lone electron pair
Copper compounds

ABSTRACT

Two new complex selenite–chlorides of strontium and copper $Sr_2Cu(SeO_3)_2Cl_2$ (I) and $SrCu_2(SeO_3)_2Cl_2$ (II) were obtained and characterized by X-ray diffraction technique, DTA and IR spectroscopy. Both compounds crystallize in the monoclinic system I: Sp. gr. $P2_1/n$, $a = 5.22996(3)$ Å, $b = 6.50528(4)$ Å, $c = 12.34518(7)$ Å, $\beta = 91.3643(2)^\circ$, $Z = 2$; II: Sp. gr. $P2_1$, $a = 7.1630(14)$ Å, $b = 7.2070(14)$ Å, $c = 8.0430(16)$ Å, $\beta = 95.92(3)^\circ$, $Z = 2$. Comparison of the crystal structure of (I) with the structures of $Sr_2M(SeO_3)_2Cl_2$ (M = Co, Ni) was performed. The substitution of strontium atom in the structure of (I) by Cu^{2+} ion with a $3d^9$ Jahn–Teller distorted surrounding leads to the lowering of the structure symmetry and to the appearance of the noncentrosymmetric structure of (II). The noncentrosymmetric character of the structure of (II) was confirmed by SHG signal (1.2 units relative to an α-quartz powder sample).

1. Introduction

Noncentrosymmetric (NCS) compounds exhibit a number of interesting and useful properties such as ferroelectricity, piezoelectricity, and second-order nonlinear optical (NLO) behavior. The asymmetric cationic coordination environment is frequently observed in NCS crystals. Two families of cations are often met in asymmetric environments: *d*-metals and lone pair ions (Sn^{2+}, Se^{4+}, Te^{4+}, etc.). In addition, the oxyhalides of the transition-metals and Se(IV) or Te(IV) display a number of new structure types and unusual magnetic properties such as low-dimensional magnetism, etc. [1–3].

In our previous work [4] the new selenite chlorides of Sr and *d*-metals (Co, Ni) were described. However, all just mentioned compounds exhibit centrosymmetric crystal structures. It is well known that copper (II) cations with the d^9 electron configuration usually provide a good example of ions with strongly distorted surrounding due to the first order Jahn–Teller effect. From this point of view incorporation of copper ions into a selenite compound may increase the probability of the NCS structure formation. However, pure copper (II) selenite–chloride exists in two polymorphs which are centrosymmetric and crystallize in $P\bar{1}$ [5] and $C2/m$ [6] space groups as well as most of copper (II) selenites, oxoselenites and diselenites [7–12]. Only one polymorph of $Cu_2O(SeO_3)$ [10] crystallizes in the NCS space group $P2_13$. The mixed metal selenite–chlorides may appear to be more appropriate for NCS formation. Moreover, the Jahn–Teller distortion of the Cu^{2+} $3d^9$ configuration may lead to the originating of important magnetic properties, such as spin ordering and spin frustrations [13–15].

In the present study we report the synthesis and structure characterization of two novel strontium–copper (II) selenite–chlorides $Sr_2Cu(SeO_3)_2Cl_2$ (**I**) and $SrCu_2(SeO_3)_2Cl_2$ (**II**).

2. Experimental section

2.1. Synthesis and structure determination

$Sr_2Cu(SeO_3)_2Cl_2$ was obtained as a green fine powder using the technique described elsewhere [4]. Strontium selenite prepared according to [16] was mixed under argon with anhydrous $CuCl_2$ (Merk > 98%) in molar ratio 2:1. The mixture was sealed in a quartz tube and heated at 550 °C for 48 h. The bulk powder sample contained a very small amount of green crystals. The X-ray powder pattern (2Θ range 10–120°, step size 0.01°, STADI P (STOE) diffractometer, transmission mode, Ge curved monochromator, Cu$K\alpha_1$ radiation, linear-PSD) from the obtained substance showed similarity to the patterns obtained from $Sr_2M(SeO_3)_2Cl_2$ (M = Co, Ni) [4]. Most of the reflections on the powder diffractogram were indexed in a monoclinic system with the parameters $a = 5.22995(2)$ Å, $b = 6.50527(3)$ Å, $c = 12.34517(7)$ Å, $\beta = 91.3641(2)^\circ$, similar to those known for $Sr_2M(SeO_3)_2Cl_2$. No contradictions with the extinctions of the $P2_1/n$ (No. 14) space group were found. The structure determination based on powder data was performed. As a model for the structure refinement, coordinates of metal, selenium and chlorine atoms were taken from the $Sr_2M(SeO_3)_2Cl_2$ structure. The refinement was carried out utilizing the JANA2000

* Corresponding author. Fax: +7 495 939 0998.
E-mail address: berdonosov@inorg.chem.msu.ru (P.S. Berdonosov).

0022-4596/$ - see front matter © 2009 Elsevier Inc. All rights reserved.
doi:10.1016/j.jssc.2009.06.020

package [17]. Thermal displacements for heavy atoms were refined anisotropically. Positions of oxygen atoms were obtained by the sequence of least-squares cycles and difference Fourier syntheses. Their thermal parameters were fitted in isotropic approximation (see supplementary materials). According to the refinement results, the formula $Sr_2Cu(SeO_3)_2Cl_2$ was assigned to the obtained compound.

Table 1
Crystal data and structure refinement for $Sr_2Cu(SeO_3)_2Cl_2$ and $SrCu_2(SeO_3)_2Cl_2$.

Formula	$Sr_2Cu(SeO_3)_2Cl_2$	$SrCu_2(SeO_3)_2Cl_2$
Sample	Powder	Single crystal
Temperature (K)		293(2)
Crystal system		Monoclinic
Space group	$P2_1/n$(#14)	$P2_1$(#4)
Cell parameters		
a (Å)	5.22996(3)	7.1630(14)
b (Å)	6.50528(4)	7.2070(14)
c (Å)	12.34518(7)	8.0430(16)
β (deg)	91.3643(2)	95.92(3)
Cell volume (Å^3)	419.894(7)	413.00(14)
Z	2	2
Calculated density (g/cm^3)	4.458	4.339
Absorption coefficient (mm^{-1})	17.902	20.984
Difractometer	Stadi-P (Stoe)	CAD4 (Nonius)
Wave lengths	Cu$K\alpha$1	Mo$K\alpha$
Θ range	$5<2\Theta<60^\circ$	$2.55<\Theta<28.00$
Reflections collected		2162
Unique reflections		2015[R(int) = 0.0477]
Ref. parameters	67	118
Software	JANA-2000 [17]	Shelx-97 [18]
Flack parameter		0.02(2)
Goodness-of-fit on F^2		1.005
χ^2	2.27	
Final R values	$R_p = 0.0376$ $R_{wp} = 0.0500$ $R_{exp} = 0.0294$	$R1 = 0.0419$, w$R2 = 0.1095$
Largest diff. peak and hole (eÅ^{-3})		1.828 and −1.280
ICSD number		420 491

The refined crystal structure seemed to be reasonable, but a small number of low intense reflections remained unindexed. Due to that a special attention was paid to a small amount of green crystals found in the obtained powder sample. A suitable crystal was mounted on a CAD-4 (Nonius) goniometer head. It was observed that the crystal should have a completely different structure from that obtained during the powder refinement, as its unit cell parameters were found to be $a = 7.163(1)$ Å, $b = 7.207(1)$ Å, $c = 8.0430(1)$ Å, $\beta = 95.92(2)^\circ$. The unit cell parameters were refined based on 24 well-centered reflections in the angular range $12.2^\circ < \theta < 13.9^\circ$. The data set was collected at ambient temperature in an ω-2θ mode with the data collection parameters listed in Table 1. A semiempirical absorption correction was applied to the data based on ψ-scans of 8 reflections having their χ angles close to 90°. Analysis of the systematic extinctions revealed two possible space groups, $P2_1$ (No. 4) and $P2_1/m$ (No. 11). The crystal structure of the compound under consideration was successfully refined in the noncentrosymmetric space group $P2_1$. Positions of all atoms except oxygen were found by direct methods (SHELXS-97) [18]. Oxygen atoms were localized by a sequence of least-squares cycles and a $\Delta\rho(xyz)$ synthesis. Final anisotropic refinement on F^2 (SHELXL-97) [18] led to $R1 = 0.0419$ and w$R2 = 0.1091$. No transition to a centrosymmetric space group was possible. After the refinement a formula $SrCu_2(SeO_3)_2Cl_2$ was assigned to the compound. Further details of the crystal structure investigation may be obtained from Fachinformationszentrum Karlsruhe, 76344 Eggenstein-Leopoldshafen, Germany (fax: (+49)7247-808-666; e-mail: crysdata@fiz-karlsruhe.de, http://www.fiz-karlsruhe.de/request_for_deposited_data.html) on quoting the CSD number 420491.

After the structure of the second phase was established, the powder pattern was immediately completely indexed as a mixture of two phases. Final refinement allowed us to establish the composition of the mixture as 98.6 wt% of $Sr_2Cu(SeO_3)_2Cl_2$ and 1.4 wt% of $SrCu_2(SeO_3)_2Cl_2$. Details of the final refinement are summarized in Table 1. The final XRD powder fit is depicted in Fig. 1.

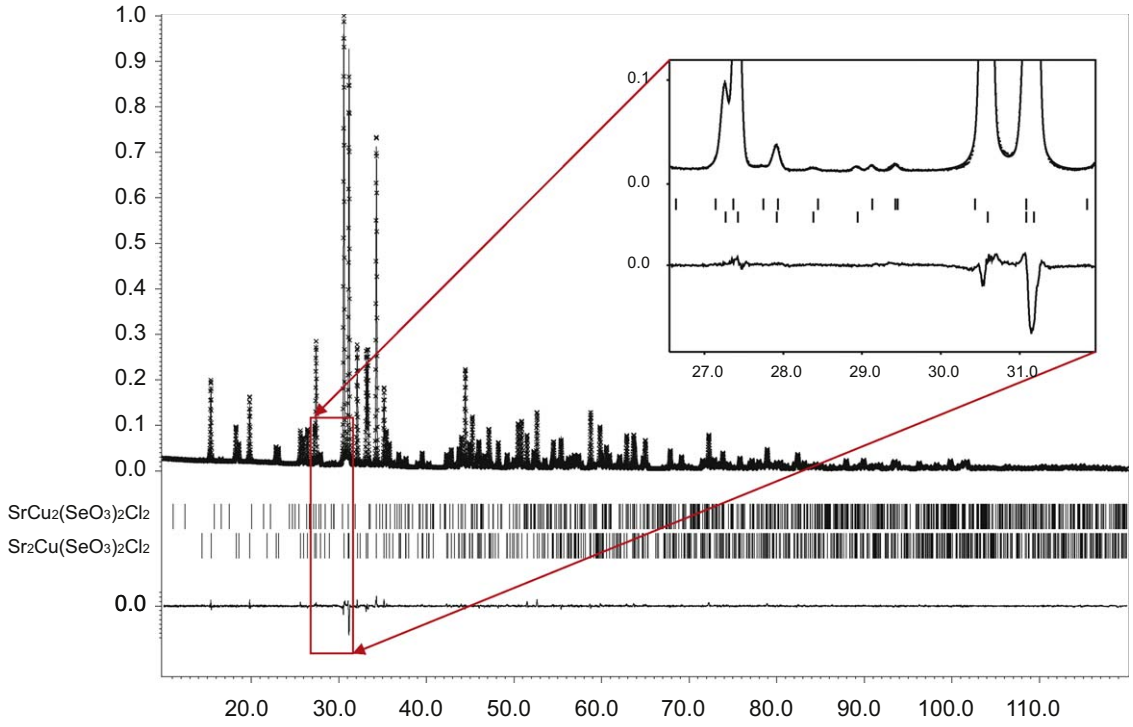

Fig. 1. Final XRD pattern fit for $Sr_2Cu(SeO_3)_2Cl_2$ structure determination experiment. The insert shows the region with the strongest $SrCu_2(SeO_3)_2Cl_2$ reflections.

The composition $SrCu_2(SeO_3)_2Cl_2$ was confirmed by direct synthesis from stoichiometric mixture of CuO (ultra pure), SeO_2 and anhydrous $SrCl_2$ obtained by calcination of $SrCl_2 \cdot 6H_2O$ (chemically pure). The mixture was heated in a sealed quartz tube for 72 h at 550 °C. The X-ray pattern from the obtained green substance (Sp. gr. $P2_1$, $a = 7.174(4)$ Å, $b = 7.217(4)$ Å, $c = 8.053(4)$ Å, $\beta = 95.83(4)^\circ$, $V = 414.8(3)$ Å^3) was in perfect agreement with the simulated one based on the results of the single crystal structure refinement.

Noncentrosymmetric character of the $SrCu_2(SeO_3)_2Cl_2$ crystal structure was verified by the SHG testing using a powder technique with the set-up similar to that employed by Kurtz and Perry [19]. A YAG:Nd-laser was used as a source of powerful impulse radiation at a wavelength $\lambda = 1.064$ μm with a repetition rate of 4 impulses per second and a duration of impulses about 10 ns. The intensity $I_{2\omega}$ of the signal at doubled frequency ($\lambda_{2\omega} = 0.532$ μm) was registered from substances in the backward direction. A measured value of the $SrCu_2(SeO_3)_2Cl_2$ grinded powder sample in relation to the SHG intensity of the α-quartz 3 μm powder is 1.2.

2.2. IR-diagnostic

IR spectra were collected using a PerkinElmer FT-IR spectrometer Spectrum One in 4000–350 cm^{-1} range. The examined substances were pressed into 0.5 mm thick pellets with KBr (Aldrich, for FTIR analysis). The substance content was 0.25–0.5 mass%. In the range of 4000–1200 cm^{-1} all the substances are transparent. Transmission IR spectra in the range of 1500–350 cm^{-1} are deposited at supplementary materials.

2.2.1. Thermal analysis

Thermal analysis of the obtained substances was performed using a NETZSCH STA 409 PC setup in air. The samples of approximately 15 mg were heated in an alumina crucible from room temperature up to 1000 °C with a speed of 10 °C/min. DTA and TG curves are presented in Fig. 2.

$Sr_2Cu(SeO_3)_2Cl_2$ is stable up to 450 °C (Fig. 2a). At this temperature the compound starts to decompose. On TG curve (Fig. 2) it is possible to see three steps at temperature ranges 520–580, 700–840 and 880–930 °C. On DTA curve (Fig. 2a) the effects were registered between TG plateaus. The transition from the second to the third TG range accompanied by three sharp DTA effects at temperatures 845, 860 and 880 °C. Total weight loss is ~18%. This value is close to 19.6%, which corresponds to the loss of one molecule of SeO_2 for a formula unit. It was not possible to determine the phase composition for the substance after DTA by X-ray analysis using ICDD PDF2 [20].

Additional experiments were performed to determine the products of different stages of $Sr_2Cu(SeO_3)_2Cl_2$ decomposition. The pure $Sr_2Cu(SeO_3)_2Cl_2$ sample was heated in air in an electrical furnace with a heating rate 10 °C/min from room temperature up to 500 °C. The sample was exposed at 500 °C for 15 min. The X-ray analysis from obtained gray powder sample revealed that it contains $SrSeO_4$ as a main crystalline phase and a small amount of Cu_2O.

The same 15 min treatment of $Sr_2Cu(SeO_3)_2Cl_2$ powder sample was made at 800 °C in air. The X-ray pattern shows the appearance of $SrSeO_3$ in the sample together with $SrSeO_4$. A small number of low intensity reflections in the pattern were not attributed to known compounds.

It is not possible to suggest simple chemical equations that would describe the weight loss for $Sr_2Cu(SeO_3)_2Cl_2$ upon heating in air. Nevertheless, it is clear that decomposition of

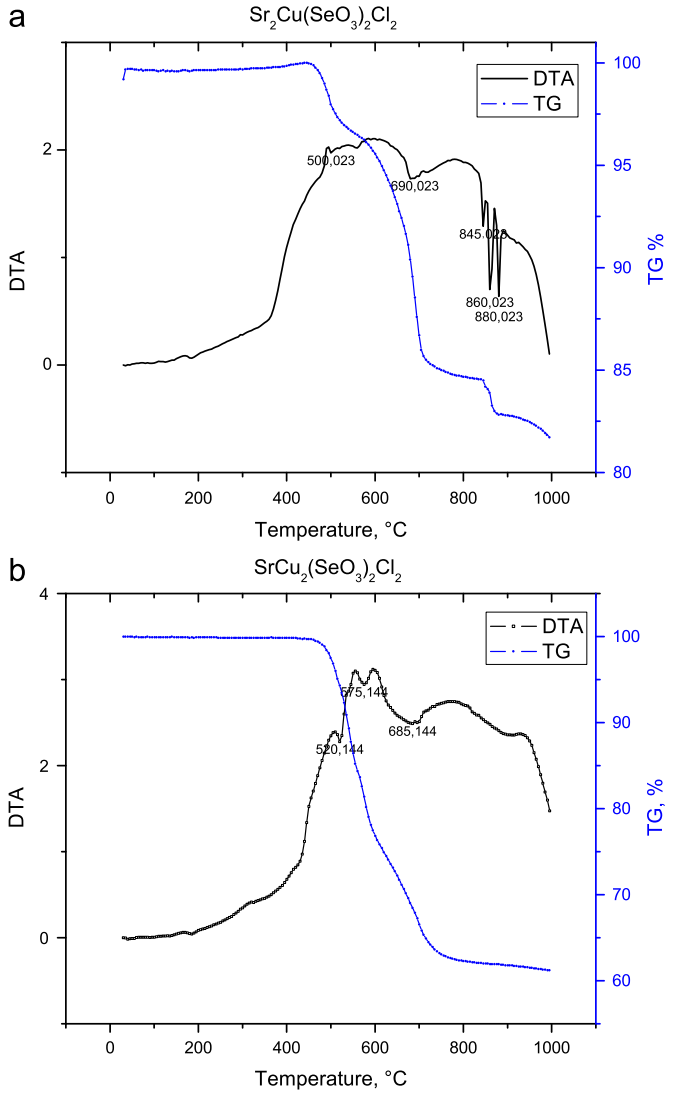

Fig. 2. TG and DTA curves for $Sr_2Cu(SeO_3)_2Cl_2$ (a) and $SrCu_2(SeO_3)_2Cl_2$ (b).

$Sr_2Cu(SeO_3)_2Cl_2$ in air is a complex process which differs much from that for $Sr_2M(SeO_3)_2Cl_2$ (M = Co, Ni) [4].

$SrCu_2(SeO_3)_2Cl_2$ starts to decompose at approximately 425 °C (Fig. 2b). The total weight loss at 1000 °C is about 39%, which corresponds to losing two SeO_2 molecules (theoretically, 41%). The second DTA effect at 575 °C corresponds to about 20% weight loss. Thus we attribute this temperature to the beginning of the second SeO_2 molecule ejection. However on the TG curve there is no well defined plateau between the first and second steps.

3. Results and discussion

Two new strontium copper selenite chlorides were obtained.

The crystal structure of $Sr_2Cu(SeO_3)_2Cl_2$ contains one crystallographically independent strontium atom, one copper and one selenium atom (Table 2).

The nearest coordination surrounding of Sr and Cu atoms comprises oxygen and chlorine atoms, whereas Se atoms have only oxygen atoms as neighbors (Table 3).

Bond valence sum [21] for Sr leads to the value of 1.94 using $[SrO_6Cl_3]$ surrounding as for $Sr_2M(SeO_3)_2Cl_2$ (M = Co, Ni) compounds. Thus, the coordination environment of strontium exhibits

Table 2
Atomic coordinates and equivalent isotropic displacement parameters ($Å^2$) for $Sr_2Cu(SeO_3)_2Cl_2$ (Sp. gr. $P2_1/n$) and $SrCu_2(SeO_3)_2Cl_2$ (Sp. gr. $P2_1$).

Atom	Site	x	y	z	U (eq)[a]
$Sr_2Cu(SeO_3)_2Cl_2$					
Cu(1)	2b	−1/2	1/2	0	0.0238(4)
Sr(1)	4e	0.01274(9)	0.28382(8)	0.23113(4)	0.0246(2)
Se(1)	4e	−0.00494(12)	0.75165(9)	0.07335(6)	0.0218(2)
Cl(1)	4e	−0.4690(2)	0.14519(17)	0.11381(11)	0.0311(6)
O(1)	4e	0.2268(5)	0.5739(4)	0.1043(2)	0.0209(9)[b]
O(2)	4e	0.0385(5)	0.9056(4)	0.1822(2)	0.0214(9)[b]
O(3)	4e	−0.2652(6)	0.6090(4)	0.1114(2)	0.0200(9)[b]
$SrCu_2(SeO_3)_2Cl_2$					
Sr(1)	2a	0.3736(1)	0.4706(2)	0.9297(1)	0.013(1)
Cu(1)	2a	0.8641(2)	0.4669(2)	0.0976(2)	0.013(1)
Cu(2)	2a	0.1985(2)	0.4844(2)	0.4112(2)	0.013(1)
Se(1)	2a	0.3720(1)	0.8197(1)	0.6173(1)	0.010(1)
Se(2)	2a	0.1449(1)	0.1141(1)	0.2140(1)	0.010(1)
Cl(1)	2a	0.3749(4)	0.7208(4)	0.2156(3)	0.019(1)
Cl(2)	2a	0.0565(4)	0.1864(4)	0.6272(3)	0.018(1)
O(1)	2a	0.0647(11)	0.3384(10)	0.2313(10)	0.013(2)
O(2)	2a	0.3577(10)	0.8494(10)	0.8283(9)	0.011(1)
O(3)	2a	0.2933(10)	0.1358(10)	0.0546(9)	0.011(1)
O(4)	2a	0.6045(10)	0.7981(11)	0.6159(10)	0.014(2)
O(5)	2a	0.3125(12)	0.5902(12)	0.6164(10)	0.017(2)
O(6)	2a	0.0315(11)	0.5317(10)	0.9258(10)	0.013(2)

[a] Ueq is defined as one third of the trace of the orthogonalized Uij tensor.
[b] Oxygen atoms were refined in isotropic approximation.

Table 3
Bond lengths (Å) for $Sr_2Cu(SeO_3)_2Cl_2$ and $SrCu_2(SeO_3)_2Cl_2$.

$Sr_2Cu(SeO_3)_2Cl_2$		$SrCu_2(SeO_3)_2Cl_2$	
Bond	Distance	Bond	Distance
Sr(1)–O(2)	2.538(3)	Sr(1)–O(6)	2.486(7)
Sr(1)–O(3)	2.621(10)	Sr(1)–O(5)	2.657(8)
Sr(1)–O(2)	2.676(10)	Sr(1)–O(3)	2.658(7)
Sr(1)–O(1)	2.711(7)	Sr(1)–O(3)	2.699(8)
Sr(1)–O(1)	2.778(10)	Sr(1)–O(2)	2.736(8)
Sr(1)–O(3)	2.945(8)	Sr(1)–O(2)	2.849(7)
Sr(1)–O(2)	3.208(10)	Sr(1)–Cl(1)	2.879(3)
Sr(1)–Cl(1)	3.232(12)	Sr(1)–Cl(1)	2.921(3)
Sr(1)–Cl(1)	3.014(12)	Cu(1)–O(1)	1.939(8)
Sr(1)–Cl(1)	3.044(2)	Cu(1)–O(2)	1.947(7)
Cu(1)–O(1) ×2	2.005(10)	Cu(1)–O(6)	1.977(7)
Cu(1)–O(3) ×2	1.955(9)	Cu(1)–O(3)	1.992(7)
Cu(1)–Cl(1) ×2	2.705(1)	Cu(1)–Cl(2)	2.732(3)
Se(1)–O(2)	1.687(3)	Cu(2)–O(5)	1.921(8)
Se(1)–O(1)	1.712(4)	Cu(2)–O(1)	1.957(8)
Se(1)–O(3)	1.722(5)	Cu(2)–O(4)	1.976(8)
		Cu(2)–Cl(2)	2.331(3)
		Cu(2)–Cl(1)	2.717(3)
		Cu(1)–Cu(2)	3.297(2)
		Se(1)–O(4)	1.674(7)
		Se(1)–O(5)	1.708(9)
		Se(1)–O(2)	1.724(7)
		Se(2)–O(6)	1.709(8)
		Se(2)–O(1)	1.726(7)
		Se(2)–O(3)	1.755(7)

a very distorted 9-vertex polyhedron (Fig. 3a).[1] Copper atoms have a usual for copper (II) distorted octahedral coordination $[CuO_4Cl_2]$ (Fig. 3b) (Table 3) with BVS ~1.975. Two chlorine atoms are situated in tans positions in $[CuO_4Cl_2]$ octahedron. Selenite groups $[SeO_3]$ possess a typical pyramidal shape with BVS = 3.93. $[SrO_6Cl_3]$ polyhedra connect to each other by common O–O or O–Cl edges and form a layer parallel to the *ab* plane of the unit cell. SeO_3 groups play a role of additional cross links for this layer. $[CuO_4Cl_2]$ octahedra are bonded to $[SrO_6Cl_3]$ polyhedra by common O–O and O–Cl edges and link layers along [001] direction into a 3D structure. The SeO_3 groups (Se–O bonds are drawn as thick lines in Fig. 4) are situated in the channels of the 3D structure (Fig. 4). This structure description is similar to such for $Sr_2M(SeO_3)_2Cl_2$ (M = Co, Ni) [4]. The structure of $Sr_2M(SeO_3)_2Cl_2$ has a center of symmetry and Cu–Cu distances are longer than 5 Å which exclude any possible spin–spin interaction between copper (II) ions.

The crystal structure of $SrCu_2(SeO_3)_2Cl_2$ is different. The symmetry of the $SrCu_2(SeO_3)_2Cl_2$ is lower (space group $P2_1$) than that for $Sr_2Cu(SeO_3)_2Cl_2$ ($P2_1/n$). There is one crystallographically independent Sr atom, two Cu, two Se and two Cl atoms in the $SrCu_2(SeO_3)_2Cl_2$ unit cell. The strontium atom environment may be described as a very distorted square antiprism (Fig. 5a) formed by six oxygen atoms being 2.4–2.85 Å apart, and two chlorine atoms at the distance of 2.9 Å $[SrO_6Cl_2]$ (Table 3). This description leads to BVS = 2.07 [21]. In contrast to $Sr_2Cu(SeO_3)_2Cl_2$, two copper atoms in $SrCu_2(SeO_3)_2Cl_2$ exhibit much stronger Jahn–Teller distortion. Both copper atoms have five neighbors. Cu(1) has a $[Cu(1)O_4Cl]$ environment, and Cu(2)–$[Cu(2)O_3Cl_2]$ with BVS 1.99 (Table 3, Fig. 5b) which form distorted square pyramids. The trigonality factor τ calculated by technique [22] for Cu(1) is 0.22 and for Cu(2) is 0.05. Thus Cu(2) pyramid is more tetragonal than Cu(1) pyramid and also this can be seen in Fig. 5b. Sr polyhedra are connected along the [010] direction by common faces formed by two oxygen and one chlorine atoms into zigzag chains. Copper square pyramids are connected into pairs by axial-equatorial fashion by pairs with a Cu(1)–Cu(2) distance being 3.297(2) Å (Table 3). The zigzag Sr polyhedra chains are stitched by Cu polyhedron pairs and SeO_3 pyramids into a 3D structure (Fig. 6). Selenium atoms have three oxygen atoms in the coordination sphere (Table 3) with BVS 4.03 for Se(1) and 3.73 for Se(2).

The comparison of IR spectra for new substances shows that $SrCu_2(SeO_3)_2Cl_2$ possesses more complex structure and lower symmetry. The IR spectrum of $Sr_2Cu(SeO_3)_2Cl_2$ is similar to IR spectra of $Sr_2M(SeO_3)_2Cl_2$ (M = Co, Ni) [4]. In the $Sr_2Cu(SeO_3)_2Cl_2$ and $SrCu_2(SeO_3)_2Cl_2$ IR spectra usual absorption bands 860–830 and near 760 cm^{-1} can be assigned to the ν(Se–O) vibrations; bands in the range 679–730 cm^{-1} are originating from ν(Se–O–Sr) vibrations [23]. However, due to the presence of two SeO_3^{2-} groups with different Se–O distances (Table 3) the ν(Se–O–Sr) part of the $SrCu_2(SeO_3)_2Cl_2$ spectrum is more complex.

The $SrCu_2(SeO_3)_2Cl_2$ crystal structure is similar to the structure of the tellurites $SrCu_2(TeO_3)_2Cl_2$ [15] and $BaCu_2(TeO_3)_2Cl_2$ [24]. It is worth noting that in the tellurite compounds Cu atoms can be considered to form a chain of weakly connected dimers which can be satisfactorily described by a Heisenberg spin model [15]. In the case of $SrCu_2(TeO_3)_2Cl_2$ and $BaCu_2(TeO_3)_2Cl_2$ the shortest Cu–Cu distance is 3.34 Å [15,24]. The selenite group has smaller dimensions which results in a shortening of the Cu–Cu distances to 3.297(2) Å (Table 3). This enables one to suggest that in $SrCu_2(SeO_3)_2Cl_2$, Cu^{2+}–Cu^{2+} spin interactions may be expected.

[1] Thermal ellipsoids on all figures are drawn with 90% probability.

Acknowledgments

This work was supported by Russian RFBR Grants 08-03-00548 and 09-03-00799. Dr. T.B. Shatalova is gratefully acknowledged for help in DTA experiment collection and Mrs. I.V. Kolesnick is acknowledged for assistance in IR spectra obtaining. Dr. S.Yu. Stefanovich is acknowledged for SHG tests. We thank Prof A.V. Shevelkov for valuable discussions.

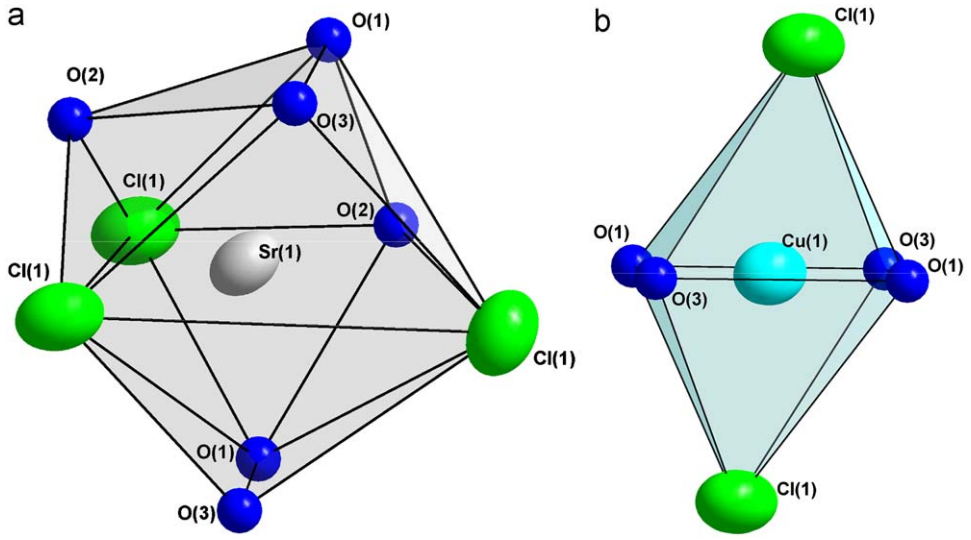

Fig. 3. (a) Coordination surrounding at Sr; (b) coordination surrounding at Cu in the $Sr_2Cu(SeO_3)_2Cl_2$ crystal structure.

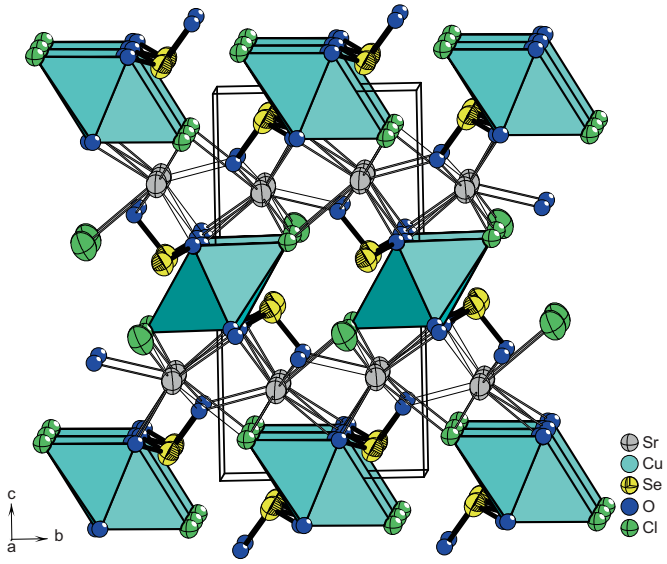

Fig. 4. The crystal structure of $Sr_2Cu(SeO_3)_2Cl_2$ presented in Cu polyhedra.

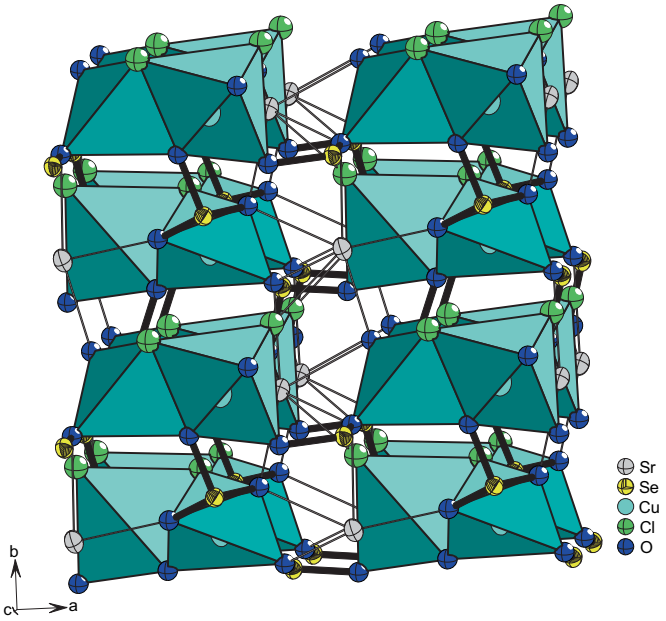

Fig. 6. The crystal structure of $SrCu_2(SeO_3)_2Cl_2$ presented in Cu polyhedra.

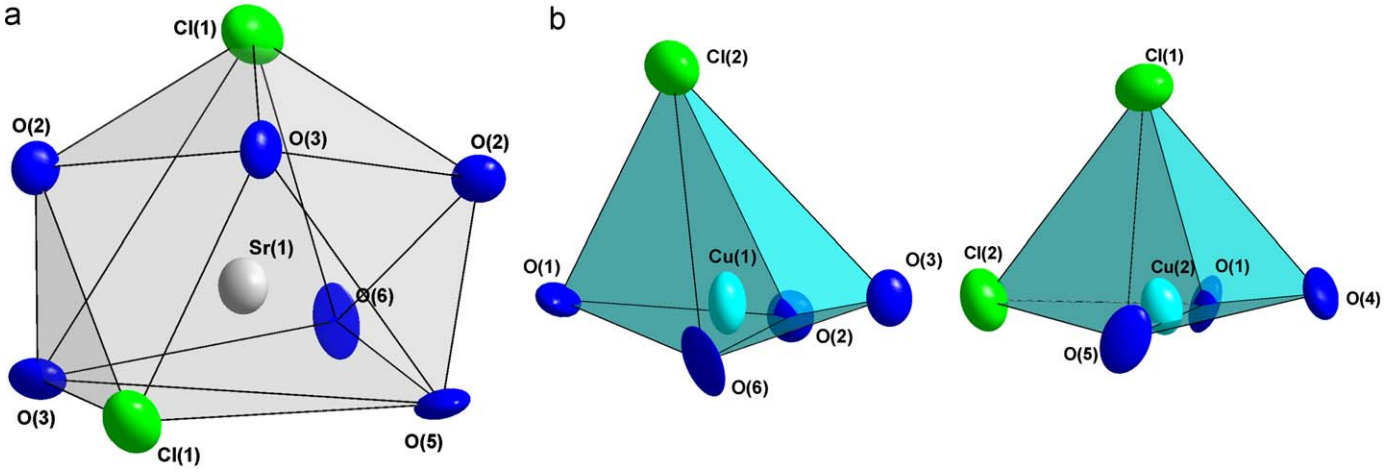

Fig. 5. Coordination surrounding of Sr (a) and Cu (b) in the $SrCu_2(SeO_3)_2Cl_2$ crystal structure.

Appendix A. Supplementary data

Supplementary data associated with this article can be found in the online version at 10.1016/j.jssc.2009.06.020.

References

[1] J.-G. Mao, H.-L. Jiang, F. Kong, Inorg. Chem. 47 (2008) 8498–8510.
[2] M. Johnsson, K.W. Törnroos, F. Mila, P. Millet, Chem. Mater. 12 (2000) 2853–2857.
[3] R. Becker, M. Johnsson, H. Berger, M. Prester, I. Zivkovic, D. Drobac, M. Miljak, M. Herak, Solid State Sci. 8 (2006) 836–842.
[4] P.S. Berdonosov, A.V. Olenev, A.N. Kuznetsov, V.A. Dolgikh, J. Solid State Chem. 182 (2009) 77–82.
[5] P. Millet, B. Bastide, M. Johnsson, Solid State Commun. 113 (2000) 719–723.
[6] R. Becker, H. Berger, M. Johnsson, Acta Cryst. C 63 (2007) i4–i6.
[7] K. Kohn, K. Inoue, O. Horie, S. Akimoto, J. Solid State Chem. 18 (1976) 27–37.
[8] G. Meunier, C. Svenssen, A. Carpy, Acta Cryst. B 32 (1976) 2664–2667.
[9] H. Effenberger, Z. Kristallogr. 175 (1986) 61–72.
[10] H. Effenberger, F. Pertlik, Monatsh. Chem. 117 (1986) 887–896.
[11] F.C. Hawthorne, T.S. Ercit, L.A. Groat, Acta Cryst. C 42 (1986) 1285–1287.
[12] R. Becker, H. Berger, Acta Cryst. E 62 (2006) i256–i257.
[13] M. Johnsson, K.W. Törnroos, F. Mila, P. Millet, Chem. Mater. 12 (2000) 2853–2857.
[14] P. Millet, B. Bastide, V. Pashchenko, S. Gnatchenko, V. Gapon, Y. Ksari, A. Stepanov, J. Mater. Chem. 11 (2001) 1152–1157.
[15] R. Takagi, M. Johnsson, R.K. Kremer, P. Lemmens, J. Solid State Chem. 179 (2006) 3763–3767.
[16] O.A. Dityatiev, P. Lightfoot, P.S. Berdonosov, V.A. Dolgikh, Acta Cryst. E 63 (2007) i149–i150.
[17] V. Petricek, M. Dusek, L. Palatinus, Jana2000. The Crystallographic Computing System, Institute of Physics, Praha, Czech Republic, 2000.
[18] G.M. Sheldrick, Acta Cryst. A 64 (2008) 112–122.
[19] S.K. Kurtz, T.T. Perry, J. Appl. Phys. 39 (1968) 3798–3813.
[20] The International Centre for Diffraction Data 12 Campus Boulevard Newtown Square, PA 19073-3273, USA. 〈http://www.icdd.com〉 PDF2, 2001.
[21] I.D. Brown, Bond valence sum parameters version 2006-05-02, 〈http://www.ccp14.ac.uk/ccp/web-mirrors/i_d_brown/bond_valence_param/bvparm2006.cif〉.
[22] A.W. Addison, T.N.J. Rao, J. Reedijk, J. van Rijn, G.C. Verschoor, J. Chem. Soc. Dalton Trans. (1984) 1349–1356.
[23] H.-L. Jiang, J.-G. Mao, J. Solid State Chem. 181 (2008) 345–354.
[24] C.R. Feger, J.W. Kolis, Inorg. Chem. 37 (1998) 4046–4051.